

# Selective antagonism of TRPA1 produces limited efficacy in models of inflammatory- and neuropathic-induced mechanical hypersensitivity in rats

Sonya G Lehto, PhD<sup>1</sup>, Andy D Weyer, DPT, PhD<sup>2</sup>, Beth D Youngblood, BS<sup>1</sup>, Maosheng Zhang, MD<sup>1</sup>, Ruoyuan Yin, MD<sup>1</sup>, Weiya Wang, MD<sup>1</sup>, Yohannes Teffera, PhD<sup>3</sup>, Melanie Cooke, MS<sup>4</sup>, Cheryl L Stucky, PhD<sup>5</sup>, Laurie Schenkel, PhD<sup>6</sup>, Stephanie Geuns-Meyer, PhD<sup>6</sup>, Bryan D Moyer, PhD<sup>1</sup>, Kenneth D Wild, PhD<sup>1</sup> and Narender R Gavva, PhD<sup>1</sup>

## Abstract

The transient receptor potential ankyrin 1 (TRPA1) channel has been implicated in pathophysiological processes that include asthma, cough, and inflammatory pain. Agonists of TRPA1 such as mustard oil and its key component allyl isothiocyanate (AITC) cause pain and neurogenic inflammation in humans and rodents, and TRPA1 antagonists have been reported to be effective in rodent models of pain. In our pursuit of TRPA1 antagonists as potential therapeutics, we generated AMG0902, a potent (IC<sub>90</sub> of 300 nM against rat-TRPA1), selective, brain penetrant (brain to plasma ratio of 0.2), and orally bioavailable small molecule TRPA1 antagonist. AMG0902 reduced mechanically evoked C-fiber action potential firing in a skin-nerve preparation from mice previously injected with complete Freund's adjuvant, supporting the role of TRPA1 in inflammatory mechanosensation. In vivo target coverage of TRPA1 by AMG0902 was demonstrated by the prevention of AITC-induced flinching/licking in rats. However, oral administration of AMG0902 to rats resulted in little to no efficacy in models of inflammatory, mechanically evoked hypersensitivity; and no efficacy was observed in a neuropathic pain model. Unbound plasma concentrations achieved in pain models were about 4-fold higher than the IC<sub>90</sub> concentration in the AITC target coverage model, suggesting that either greater target coverage is required for efficacy in the pain models studied or TRPA1 may not contribute significantly to the underlying mechanisms.

## Keywords

TRPA1, inflammatory, neuropathic, pain, AMG0902, rat

Date received: 4 August 2016; revised: 21 September 2016; accepted: 6 October 2016

## Introduction

The transient receptor potential ankyrin 1 (TRPA1) is a nonselective cation channel implicated in noxious cold and mechanosensation that is activated by a wide variety of reactive chemicals including the active component in mustard oil, allyl isothiocyanate (AITC).<sup>1,2</sup> TRPA1 is highly expressed in small- and medium-sized nociceptive neurons of the dorsal root, trigeminal, and nodose ganglia.<sup>3–5</sup> Skin application of mustard oil causes pain in humans, and intraplantar injection of AITC causes pain-like behaviors in rodents through the activation of peripheral nerve fibers.<sup>6,7</sup> In a study with TRPA1

<sup>1</sup>Department of Neuroscience, Amgen Inc, Thousand Oaks, CA, USA

<sup>2</sup>School of Physical Therapy, Pacific University, Hillsboro, OR, USA

<sup>3</sup>Department of Pharmacokinetics and Drug Metabolism, Amgen Inc, Thousand Oaks, CA, USA

<sup>4</sup>Department of Pharmaceuticals, Amgen Inc, Thousand Oaks, CA, USA

<sup>5</sup>Department of Cell Biology, Neurobiology and Anatomy, Medical College of Wisconsin, Milwaukee, WI, USA

<sup>6</sup>Medicinal Chemistry, Amgen Inc, Cambridge, MA, USA

### Corresponding author:

Sonya G Lehto, Amgen Inc, One Amgen Center Drive, Thousand Oaks, CA 91320, USA.

Email: slehto@amgen.com



wild-type (WT) and knockout (KO) mice, it was reported that AITC did not cause pain-like behaviors in the KO mice, suggesting that TRPA1 activation is exclusively responsible for these actions.<sup>8</sup> Further, a human genetic study reported that a gain-of-function mutation in TRPA1 causes an episodic pain syndrome in which debilitating upper-body pain can be triggered by stressors.<sup>9</sup> Additionally, increased TRPA1 expression<sup>4,10,11</sup> and increases in endogenous ligands (e.g., 4-hydroxynonenal<sup>12</sup>) after inflammatory insult or nerve injury may result in mechanical hyperalgesia and cold hyperalgesia/allodynia.

Antisense knockdown of TRPA1 was reported to alleviate cold hyperalgesia after spinal nerve ligation in rodents, pointing to antagonism as a potential therapeutic approach.<sup>13</sup> Pharmacological blockade of TRPA1 by first-generation antagonists (e.g., AP18 and HC030031) was reported to be efficacious in complete Freund's adjuvant (CFA), spinal nerve ligation (SNL), and bladder hyperalgesia models.<sup>14–17</sup> Our excitement was built for the pursuit of TRPA1 as a pain therapeutic target based on its expression, human genetics, and reported efficacy with tool antagonists. However, target validation with these small molecules exhibiting weak potency and/or poor pharmacokinetic properties was challenging due to unknown off-target effects, so we set out to generate a potent, selective, and orally bioavailable compound. Here, we describe the characterization of AMG0902, 1-((3-(4-Chlorophenethyl)-1,2,4-oxadiazol-5-yl)methyl)-7-methyl-1*H*-purin-6(7*H*)-one, which has excellent target coverage in vivo<sup>18</sup> and the use of AMG0902 in the assessment of the therapeutic potential of TRPA1 antagonists for chronic pain in models of inflammatory and neuropathic pain. AMG0902 reduced mechanically evoked C-fiber action potential firing in a skin-nerve preparation from mice previously injected with CFA and produced a modest effect in CFA-induced mechanical hyperalgesia, but little to no efficacy in models of inflammatory, mechanically evoked hypersensitivity, and no efficacy was observed in a neuropathic pain model.

## Methods

### Compounds and reagents

AMG09020, synthesized at Amgen Inc (Cambridge, MA), resulted from an internal medicinal chemistry effort.<sup>18</sup> All cell culture reagents were purchased from Invitrogen (Carlsbad, CA).

### In vitro characterization

**Luminescence readout assay for measuring intracellular calcium.** Stable Chinese hamster ovary (CHO) cell lines

expressing rat TRPA1, rat transient receptor melastatin 8 (rTRPM8), rat transient receptor vanilloid 3 (rTRPV3), and human transient receptor vanilloid 4 (hTRPV4) were generated using the tetracycline inducible T-REx<sup>TM</sup> expression system from Invitrogen, Inc (Carlsbad, CA), and a stable CHO cell line expressing rat TRPV1 was generated using a constitutive expression system.<sup>19</sup> To enable a luminescence readout based on intracellular increase in calcium,<sup>20</sup> each cell line was also co-transfected with pcDNA3.1 plasmid containing jelly-fish aequorin cDNA. Twenty-four hours before the assay, cells were seeded in 96-well plates, and all TRP channel expression, except for TRPV1, was induced with 0.5 µg/ml tetracycline. On the day of the assay, culture media were removed and cells were incubated for 2 h with pH 7.2 assay buffer (F12 containing 30 mM HEPES for TRPV1, TRPA1, TRPM8, and TRPV3; F12 containing 30 mM HEPES, 1 mM CaCl<sub>2</sub>, and 0.3% BSA for TRPV4) containing 15 µM coelenterazine (P.J.K GmbH, Germany). AMG0902 was added 2.5 min prior to the addition of an agonist. Luminescence was measured by a CCD camera-based FLASH-luminometer built by Amgen Inc. The following agonists were used to activate TRP channels: 0.5 µM capsaicin for TRPV1, 80 µM AITC for TRPA1, 35 µM for 4-ONE, 2.74 methylglyoxal, 100 mOsmol for hypo-osmolarity, 1 µM icilin or cold buffer (12°C) for TRPM8, 200 µM aminoethoxydiphenyl borate (2-APB) for TRPV3, and 1 µM 4α-phorbol 12,13-didecanoate (4α-PDD) for TRPV4. Antagonist IC<sub>50</sub> values were calculated using GraphPad Prism 5.01 (GraphPad Software Inc, San Diego, CA).

**Agonist-induced <sup>45</sup>Ca<sup>2+</sup> uptake assay.** All antagonist <sup>45</sup>Ca<sup>2+</sup> uptake assays were conducted as reported previously,<sup>21</sup> with a final <sup>45</sup>Ca<sup>2+</sup> concentration of 10 µCi/mL. Two days prior to the assay, cells were seeded in Cytostar 96-well plates (Amersham) at a density of 20,000 cells/well. The activation of TRPA1 was followed as a function of cellular uptake of radioactive calcium (<sup>45</sup>Ca<sup>2+</sup>) upon cold or icilin stimulation. To determine the ability to block agonist activation of TRPA1, AMG0902 was incubated with cells for 2 min before the addition of agonist. Cells were washed after a further incubation of 2 min and the <sup>45</sup>Ca<sup>2+</sup> uptake was determined. Radioactivity was measured using a MicroBeta Jet (Perkin-Elmer Inc.).

### Pharmacokinetics in plasma and brain

Plasma pharmacokinetics of each compound in male Sprague-Dawley rats (n=3 animals per study) were determined after intravenous dosing at 2 mg/kg in 100% dimethylsulfoxide (DMSO), or after the administration of 30 mg/kg by oral gavage with test article

formulated in 1% Tween 80/2% HPMC/97% water/methanesulfonic acid pH 2.2. At designated time points, blood was collected via the femoral artery and processed for plasma by centrifugation. Plasma was then transferred into a 96-well container and stored at  $-70^{\circ}\text{C}$  until analysis. Similar bioanalytical methods were used to determine plasma and brain exposure in animals tested in pharmacodynamic and pain models. Brain samples were homogenized with a 4:1 ratio of water (mL) for every gram of brain tissue. All analytical methods utilized protein precipitation, with the addition of a structurally similar compound to function as an internal standard. Calibration standards were prepared from a 1-mg/mL stock solution of each compound in DMSO with a serial dilution into a blank matrix (plasma or brain homogenate). Liquid chromatography with tandem mass spectrometry was used for the quantitation of each compound in rat plasma and brain. Noncompartmental pharmacokinetic analysis of plasma concentrations was conducted using WinNonlin Enterprise v.5.1.1 (Pharsight Corporation, Mountain View, CA). Brain uptake was calculated as a ratio of concentration in whole brain tissue to that in plasma taken from the same animal at approximately the same time.

### Plasma protein binding

The unbound fraction in plasma was determined by ultracentrifugation. Test compound ( $5\ \mu\text{g}/\text{mL}$ ) was incubated in plasma from male rats at  $37^{\circ}\text{C}$  for 15 min. Samples were transferred to a centrifuge tube and centrifuged at  $16,128 \times g$  for 3 h at  $37^{\circ}\text{C}$ . After protein precipitation using acetonitrile containing an internal standard, supernatants were dried under a stream of nitrogen gas, with residues reconstituted in methanol/water (50:50, v/v) prior to analysis by liquid chromatography with tandem mass spectrometry. The concentration was determined from a linear regression of peak area ratios (analyte peak area/internal standard peak area) relative to calibration standards. The unbound fraction in plasma ( $C_u$ ) was calculated as a ratio of the concentration measured relative to the nominal concentration.

### Skin nerve preparation and fiber analysis

**Evaluation of TRPA1 KO versus WT mice.** In an Amgen lab, saphenous nerve C-fibers that innervate skin were isolated from female 7- to 11-week-old littermate TRPA1 KO and WT mice<sup>22</sup> and were evaluated for mechanically induced action potential firing as previously described.<sup>23</sup> Nerve recordings and data analyses were conducted in a blinded manner with respect to genotype.

**Evaluation of AMG0902.** In a lab at the Medical College of Wisconsin, the mouse saphenous skin-nerve in vitro preparation<sup>24-26</sup> was used for electrophysiological recordings of cutaneous terminals of primary afferent fibers in situ. Recordings were conducted on adult (7–18 weeks of age), male mice injected with  $30\ \mu\text{L}$  of CFA (Sigma-Aldrich, St. Louis, MO) into the left hind paw 42–54 h prior to the recordings. This time point corresponds to the second day post-injection, which has previously been found to be the day of greatest mechanical sensitivity after CFA injection.<sup>27</sup> To begin, mice were anesthetized under isoflurane-induced anesthesia and sacrificed by cervical dislocation. The hairy skin of the left hind paw was quickly dissected along with the innervating saphenous nerve. The preparation was then placed corium side up in a bath containing oxygenated buffer consisting of the following (in mM): 123 NaCl, 3.5 KCl, 0.7  $\text{MgSO}_4$ , 1.7  $\text{NaH}_2\text{PO}_4$ , 2.0  $\text{CaCl}_2$ , 9.5 sodium gluconate, 5.5 glucose, 7.5 sucrose, and 10 HEPES. The buffer was titrated to a pH of  $7.45 \pm 0.05$ , and the bath temperature during recording sessions was set to  $32.0 \pm 0.5^{\circ}\text{C}$ .

The innervating saphenous nerve was then placed on a mirror plate in a separate chamber containing mineral oil and Ag recording electrode. Next, the nerve was teased apart into fine filaments and placed on the recording electrode. A mechanical search technique was employed to stimulate the preparation and identify mechanically sensitive single-unit sensory afferents, and their activity was digitized and displayed on an oscilloscope. Once a single unit was identified, the most sensitive part of its receptive field was pinpointed and its conduction velocity calculated using electrical stimulation. Only those fibers with conduction velocities less than 1.2 m/s were used for this study, as these fibers have been identified as C fibers in the mouse.<sup>24,25</sup> von Frey filaments (0.044 to 147 mN) were used to categorize the mechanical threshold of each fiber. Fibers were grouped based on their adaptation responses to mechanical stimuli (either rapid or slow); all C fibers used in this study exhibited action potential firing throughout the duration of the mechanical stimulus and were thus classified as slowly adapting.

The receptive field of these C fibers was isolated from the surrounding buffer using a metal ring (inner diameter = 4.67 mm, outer diameter = 6.37 mm). Buffer inside the ring was then removed and replaced with buffer containing AMG0902 ( $11\ \mu\text{M}$ , 0.11% DMSO) or vehicle (0.11% DMSO) for 10 min. During the last 2 min of this incubation, baseline recordings were made with LabChart 5 software using a PowerLab data acquisition system to determine the extent of spontaneous activity (if any) exhibited by the fiber. Fibers were activated mechanically using a feedback-controlled, computer-driven mechanical stimulator with a flat ceramic tip (diameter = 0.8 mm). Increasing mechanical forces (5, 10, 20,

40, 100, 150, and 200 mN) were applied to the receptive field in the presence of AMG-0902 or buffer for 10 s, and the resulting action potentials were recorded in LabChart. One-minute intervals were given between stimuli to prevent sensitization/desensitization of fibers. All recordings and data analyses were performed with the experimenter blinded to the treatment (compound or vehicle) used.

### *In vivo pharmacodynamic and pain models*

*Studies conducted at Amgen Inc*—Adult male Sprague Dawley rats weighing 220–300 g (Harlan, San Diego) and adult TRPA1 KO and WT mice were obtained from Harvard Medical School, Boston, MA, and cared for in accordance with the Guide for the Care and Use of Laboratory Animals, 8th edition.<sup>28</sup> Animals were group-housed at an Association for Assessment and Accreditation of Laboratory Animal Committee accredited facility in non-sterile-ventilated micro-isolator housing on corn cob bedding. All research protocols were approved by the Institutional Animal Care and Use Committee. Animals had ad libitum access to pelleted feed (Harlan Teklad 2020X, Indianapolis, IN) and water (on-site-generated reverse osmosis) via automatic watering system. Animals were maintained on a 12:12 h light: dark cycle in rooms at  $21 \pm 3^\circ\text{C}$ ,  $50 \pm 20\%$  room humidity, and had access to enrichment opportunities (nesting materials and plastic domes). All animals were sourced from approved vendors who meet or exceed animal health specifications for the exclusion of specific pathogens (i.e., mouse parvovirus, Helicobacter). Animals were allowed at least one week acclimation to the facility prior to any procedures. Following completion of behavioral measurements, animals were euthanized with carbon dioxide followed by immediate blood collection via cardiac puncture for pharmacokinetic analysis. All behavioral data were scored by an observer blind to dosing condition or through an automated device. The dosing schedule was composed ahead of time and randomized such that the observer could not predict which animals were included in the same dosing group. For all in vivo models, the TRPA1 antagonist AMG0902 was formulated in 1% Tween80/2% HPMC/97% water/methanesulfonic acid pH 2.2.

*Studies conducted at the Medical College of Wisconsin*—Adult (7–18 weeks) male C57BL/6 mice were obtained from Jackson Laboratories and used for ex vivo skin-nerve preparations. Mice were allowed to acclimate to the animal facility at the Medical College of Wisconsin, an Association for the Assessment and Accreditation of Laboratory Animal Committee-accredited facility, for approximately one week following shipment. Animals were housed with up to four other cagemates and had ad libitum access to food pellets

and hyper-chlorinated water. Mice were housed on a 14:10 h light:dark cycle in cages containing aspen bedding and paper nesting material. Room temperatures averaged  $21^\circ\text{C}$ . All procedures were approved by the Institutional Animal Care and Use Committee at the Medical College of Wisconsin. Nerve recordings and data analyses were conducted in a blinded manner with respect to drug treatment.

*AITC-induced licking model.* AMG0902 (0.3, 1, 3, or 10 mg/kg) or vehicle control was administered p.o. 60 min prior to intraplantar injection of 30  $\mu\text{l}$  of AITC (0.1% in 0.5% Tween 80 and  $1 \times \text{PBS}$ ; Sigma). The number of flinches and/or guard/licks greater than 3 s was counted for a duration of 1-min post-injection. Rats were viewed through transparent Plexiglas<sup>®</sup> observation cylinders that were placed on a custom, opaque, plastic apparatus such that rats could not view each other. The dose of AITC was chosen based on an in-house dose-response effect over 0.01–3.0% in which 1% AITC was the dose that was the most approximate to the calculated  $\text{ED}_{80}$ .

*Open field activity.* Rats were habituated in a reversed light cycle room in home cages for at least one week and acclimated to the testing room for 1 h prior to dosing. AMG0902 (30, 100, or 300 mg/kg) or vehicle was administered 1 h before placing an animal in the open-field apparatus. Open-field activity was measured using a system that counts interruptions of a set of photobeams over the course of 60 min (Kinder Scientific, Poway, CA). To begin a session, animals were removed from the home cage and placed individually into an independent Plexiglas box (41 cm L  $\times$  41 cm W  $\times$  38 cm H) surrounded by a frame consisting of 32 photocells (16 Y and 16X) that track the movement of the animal. Photobeam breaks were used as an indication of activity and were measured as the following parameters per minute: basic movements (beam breaks), distance traveled (cm), time spent (s), and number of repetitive beam breaks (i.e., stereotypic movement). Gabapentin, which consistently elicits a decrease in open field activity, was used as a positive control. Gabapentin was formulated in the same vehicle as AMG0902 at 200 mg/kg p.o. and also dosed 1 h before the start of the open field assay.

*CFA-induced hypersensitivity. Decreased rearing in an open field assay*—Rats were habituated to a reversed light cycle room for at least one week and to the testing room for 1 h prior to dosing. To begin the study, rats received an injection of CFA into the left hind paw (100  $\mu\text{l}$  of 50% CFA in saline) based on previous demonstration that this causes a decrease in rearing. Since this rearing deficit can be significantly reversed by treatment with indomethacin, it is presumed to represent mechanical and/or tactile hypersensitivity with rats

rearing less in order to avoid weight bearing on the inflamed hind paw.<sup>29</sup> Twenty-one hours after the CFA injection, rats were treated (p.o.) with vehicle or TRPA1 antagonist at 10, 30, or 100 mg/kg. One hour after drug dosing (23 h after CFA injection), rats were placed in the same open field boxes as described above. Rearing time and rearing counts were measured for 60 min. Naproxen at a dose of 3 mg/kg dosed p.o. in the same vehicle was chosen as a positive control based on reliable efficacy demonstrated in previous experiments.<sup>29</sup>

**Hypersensitivity to paw pressure with Randall Selitto**—Rats received an injection of CFA into the left hind paw (50  $\mu$ l of 50% CFA in saline). Twenty-one hours after the CFA injection, rats were evaluated for mechanical hypersensitivity using the Digital Paw Pressure Randall Selitto Meter (IITC Life Sciences, Woodland Hills, CA). Rats exhibiting a withdrawal threshold of less than 60 g were treated (p.o.) with vehicle, AMG0902 at 300 mg/kg or indomethacin at 3 mg/kg 1 h prior to the evaluation of mechanical hypersensitivity.

**Sciatic nerve ligation (SNL)-induced tactile allodynia.** SNL surgery was performed using aseptic surgical techniques and a stereomicroscope.<sup>30</sup> Spinal nerve injury was caused by ligating the left L5 and L6 spinal nerves, with special care to avoid damage to the L4 spinal nerve or surrounding area. More specifically, under gaseous anesthesia with a mixture of O<sub>2</sub> and isoflurane (3% for induction and 2% for maintenance), skin was excised and the longissimus lumborum muscle, part of articular processes (L4-S1), and the fascia above L6 spinal nerve were carefully removed. This procedure provided a clean and spacious working area to enable complete resection of the L6 transverse process and to separate the L5 spinal nerve from the L4 spinal nerve without damage to L4. The L5 and L6 spinal nerves were each tightly ligated with 6-0 silk thread and then L5 was cut. The entire surgical procedure beginning with anesthesia and ending with wound clipping of the outside skin lasted 15 min or less.

**Behavioral testing**—Two weeks post-surgery, mechanical sensitivity was measured by determining the median 50% foot withdrawal threshold for von Frey filaments using the up-down method.<sup>31</sup> Rats were placed under a plastic cover (9  $\times$  9  $\times$  20 cm) on a metal mesh floor. von Frey filaments (Semmes-Weinstein monofilaments from Stoelting) were applied to the middle glabrous area between the footpads of the plantar surface of the injured hind paw. This plantar area was touched with a series of nine recently calibrated von Frey filaments with approximately exponentially incremental bending forces (von Frey filament numbers: 3.61, 3.8, 4.0, 4.2, 4.41, 4.6, 4.8, 5.0, and 5.2; equivalent to: 0.41, 0.63, 1.0, 1.58, 2.51, 4.07, 6.31, 10, and 15.8 g). The von Frey filament was presented perpendicular to the plantar surface with

sufficient force to cause slight bending and held for approximately 3–4 s. To avoid possible reflex responses, only abrupt withdrawal of the foot accompanied by pain indicative behaviors (namely paw flinching, shaking, or licking for more than 2 s) was recorded as a response. Any post-surgery rat that displayed a mechanical threshold of more than 3.16 g or less than 0.7 g was eliminated from the study. After measuring basal threshold, animals were treated (p.o.) with vehicle or AMG0902 (100 or 300 mg/kg), or gabapentin (200 mg/kg; Sigma, St. Louis). Measurement of the tactile threshold was reassessed at 1 and 2 h after drug administration in the same animals.

**Statistical analyses.** In vivo IC<sub>50</sub> and IC<sub>90</sub> estimates using AITC model data were determined by fitting a sigmoidal dose-response curve to individual animal response versus resulting plasma concentration. Behavioral and electrophysiological data are expressed as mean  $\pm$  standard error of the mean (SEM). Skin-nerve data were compared using a two-way analysis of variance (ANOVA). A Bonferroni post-hoc analysis was then completed to determine significance levels for individual forces. Behavioral results were analyzed using one-way ANOVA with Dunnett's multiple comparisons post-hoc test for significance relative to vehicle. Since the von Frey filament set was calibrated on a logarithmic scale by the vendor (Stoelting), our selection of nine filaments for the up-down method was also based on nearly equal logarithmic intervals,<sup>32</sup> and because it is our experience that variability noticeably increases with threshold value, data were analyzed following logarithmic transformation prior to statistical analysis. Actual gram values were plotted on a logarithmic scale Y-axis of the figures for convenience. Statistical calculations and graphs were made using GraphPad Prism 5.01 (GraphPad Software Inc, San Diego, CA). Responses of C fibers to increasing mechanical forces under vehicle or antagonist conditions were compared using a two-way ANOVA with a Bonferroni post-hoc analysis.

## Results

### *AMG0902 acts as a potent and selective TRPA1 antagonist in vitro*

TRPA1 antagonist hits were identified by high-throughput screening of Amgen's compound collection and subsequent medicinal chemistry efforts yielded AMG0902.<sup>18</sup> AMG0902 inhibits TRPA1 activation (in stably expressing CHO cells) by different chemical and physical stimuli in a concentration-dependent manner (Figure 1). AMG0902 blocked activation of rat TRPA1 via AITC (IC<sub>50</sub> = 68  $\pm$  38 nM), 4-oxo-2-nonenal (4-ONE; IC<sub>50</sub> = 585  $\pm$  110 nM), hypo-osmolarity (IC<sub>50</sub> = 10  $\pm$  2 nM),

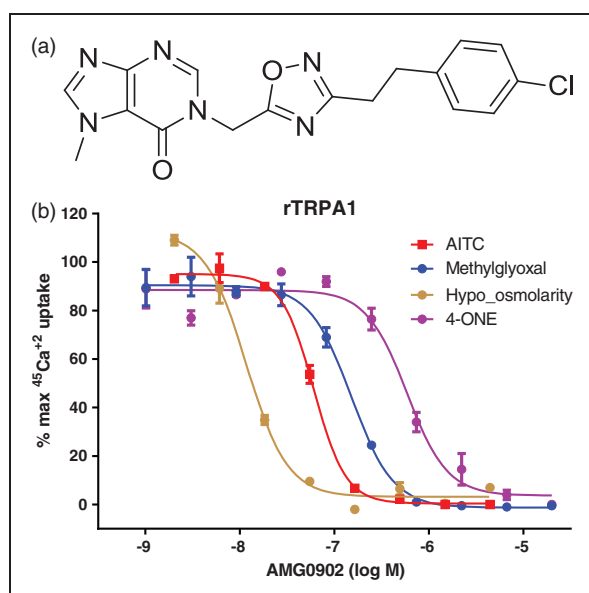


**Figure 1.** (a) Structure of AMG0902. (b) AMG0902 inhibits TRPA1 activation in stably expressing CHO cells by different chemical (80  $\mu$ M AITC; 35  $\mu$ M 4-ONE; 2.74 mM Methylglyoxal) and physical stimuli (100 mOsmol hypo-osmolarity) in a concentration-dependent manner. The maximum  $^{45}\text{Ca}^{2+}$  uptake induced by each agonist alone is considered as 100%. AITC: allyl isothiocyanate.

**Table 1.** Summary of AMG0902 properties (where indicated using mean  $\pm$  standard deviation).

Assay	AMG0902
rTRPA1 (AITC) $\text{IC}_{50}$ (nM)	68 $\pm$ 38
rTRPA1 (Osmol) $\text{IC}_{50}$ (nM)	9.7 $\pm$ 2
rTRPA1 (4-ONE) $\text{IC}_{50}$ (nM)	585 $\pm$ 110
rTRPA1 (Methylglyoxal) $\text{IC}_{50}$ (nM)	151 $\pm$ 5
rTRPA1 agonism $\text{IC}_{50}$ (nM)	>25,000
rTRPV1, V3, M8), hTRPV1, V4) $\text{IC}_{50}$ (nM)	>10,000
Rat clearance (L/h/kg)	2.5
Oral Bioavailability (%)	60
B/P ratio	0.2
Rat protein binding	71%
Rat AITC PD model $\text{IC}_{90}$ (nM)	1700

and methylglyoxal ( $\text{IC}_{50}$  = 151  $\pm$  5 nM, see Table 1). AMG0902 was also a potent antagonist of mouse ( $\text{IC}_{50}$  = 113  $\pm$  77 nM) and human ( $\text{IC}_{90}$  = 186  $\pm$  18 nM) TRPA1 activation by AITC. The in vitro potency of AMG0902 was >10  $\mu$ M at r/hTRPV1, rTRPV3, hTRPV4, and rTRPM8 and 40 targets including GPCRs, ion channels, and kinases profiled at CEREP (<33% inhibition of specific ligand binding to each target).

### TRPA1 genetic deletion or acute inhibition reduces mechanically evoked firing in cutaneous C-fibers

Ex vivo skin-nerve preparation experiments were conducted to compare how genetic deletion of TRPA1 and acute pharmacological blockade of TRPA1 with a small molecule antagonist affect mechanically induced primary afferent C-fiber activity in adult mice. Raw traces can be seen in Figure 2(a). Blinded studies demonstrated that saphenous nerve cutaneous C-fiber spiking was significantly reduced in homozygous TRPA1 KO mice at mechanical stimulation forces greater than 100 mN (Figure 2(b)), mirroring previous reports.<sup>26</sup> AMG0902 (11  $\mu$ M—a concentration that is 6.5-fold over the unbound in vivo  $\text{IC}_{90}$  from the AITC-induced finch model described below)—was next evaluated in saphenous nerves from mice two days after hind paw CFA injection. AMG0902 significantly reduced mechanically induced firing in C fibers by an average of 59% compared to DMSO vehicle controls when forces greater than 100 mN were applied (Figure 2(c)). These data indicate that acute TRPA1 inhibition decreases mechanically induced action potential firing in cutaneous C fibers. Notably, the reduction in spiking frequency at mechanical forces over 100 mN is comparable when TRPA1 function is abrogated genetically with TRPA1 knockouts or pharmacologically with the small molecule antagonist AMG0902.

### AMG0902 exhibits suitable pharmacokinetic properties for in vivo studies

In male Sprague-Dawley rats, AMG0902 provided high unbound concentrations despite high plasma clearance of 2.5 L/h/kg due to low protein binding and good oral bioavailability of 60% (as determined with a 30 mg/kg dose; see Table 1 and Schenkel et al.<sup>18</sup>). We have used unbound plasma concentrations ( $C_u$ ) to calculate the target coverage since the “protein-bound” fraction is considered unavailable for TRPA1 antagonism/occupancy.

### AMG0902 dose dependently inhibits AITC-induced licking/flinching in rats

In addition to reducing mechanically evoked action potential firing in primary afferents, AMG0902 also demonstrated efficacy in an AITC-induced licking/flinching model in rats that was used to demonstrate target coverage/engagement by TRPA1 antagonists<sup>18</sup>). AMG0902 dosed at 1, 3, 10, and 30 mg/kg exhibited dose-dependent prevention of AITC-induced licking/flinching (see Figure 5 in Schenkel et al.<sup>18</sup>). The calculated unbound mean in vivo  $\text{IC}_{90}$  for this assay was 1.74  $\pm$  0.15  $\mu$ M.<sup>18</sup>

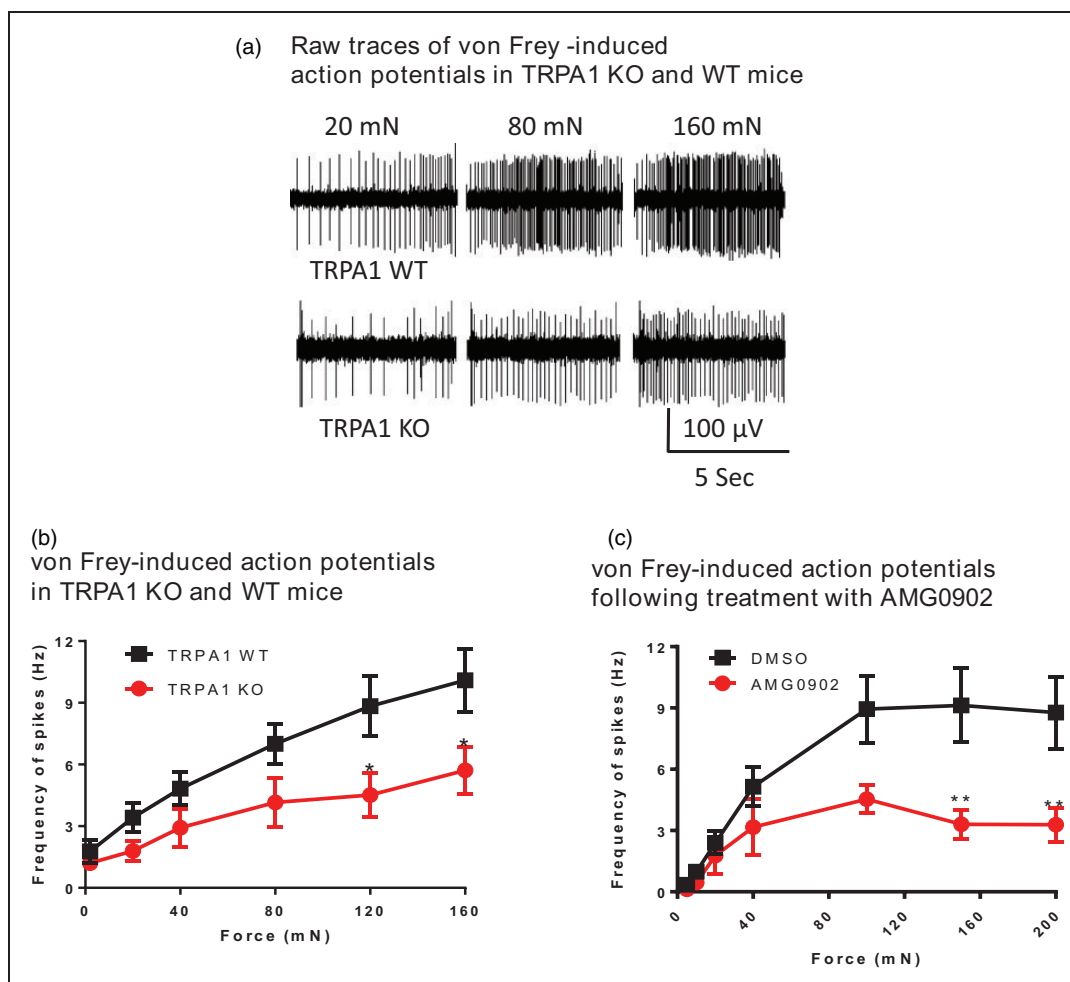


**Figure 2.** Mechanically induced C-fiber action potentials are reduced in TRPA1 knockout mice and by AMG0902 in C57BL/6 mice. (a) Representative mechanically evoked action potentials in WT and KO mice. Upper trace shows response from a single fiber in a TRPA1 WT preparation; lower trace shows responses from a single fiber in a TRPA1 KO preparation to the indicated mechanical forces (mN). (b) Frequency of C-fiber spiking was significantly reduced in TRPA1 KO mice (circles;  $n = 22$  fibers from 12 mice) compared to TRPA1 WT mice (squares;  $n = 24$  fibers from 12 mice) at 120 mN and 160 mN mechanical stimulation forces (mean  $\pm$  SEM, two-way ANOVA;  $p < 0.05$ ). (c) Frequency of C-fiber spiking was significantly reduced by 11  $\mu$ M AMG0902 (circles;  $n = 11$  fibers from three CFA-treated mice) compared to DMSO vehicle (squares;  $n = 12$  fibers from four CFA-treated mice; mean  $\pm$  SEM, two-way ANOVA;  $p < 0.01$ ). WT: wild type; KO: knockout.

### AMG0902 reduces rearing time but not distance traveled endpoints of open field activity at 300 mg/kg

During assessment of the potential analgesic effects of a compound, conclusions can be confounded by sedative or motor side effects caused by the compound, resulting in a false positive. Thus, prior to testing in inflammatory or neuropathic behavioral models, we evaluated AMG0902 in an open field assay along with a positive control of 200 mg/kg, p.o. gabapentin (expected to reduce rearing but not total distance traveled; Figure 3(a) and (b)). When AMG0902 was administered at 300 mg/kg (mean Cu concentration was  $12.6 \pm 5.4 \mu$ M;  $>7$ -fold in excess of the in vivo  $IC_{90}$  calculated from the AITC target coverage model), total distance traveled was  $7437 \pm 900$  cm, which was not significantly different

relative to the vehicle-treated group ( $9819 \pm 832$  cm;  $F_{4,35} = 1.2$ ,  $p > 0.05$ ; Figure 3(a)). When AMG0902 was administered at 300 mg/kg, rearing time was  $308 \pm 67$  s, which was significantly different relative to the vehicle-treated group ( $644 \pm 59$  s;  $F_{4,35} = 5.0$ ,  $p < 0.05$ ; Figure 3(b)). As expected, total distance traveled was not significantly reduced in rats receiving gabapentin ( $p > 0.05$ ), but rearing was significantly reduced ( $p < 0.05$ ; Figure 3(a) and (b)).

### Effect of AMG0902 on CFA-induced mechanical hypersensitivity

**No reversal of rearing deficit.** We previously validated an automated, high-throughput assay to measure spontaneous/ongoing mechanical hypersensitivity.<sup>29</sup> In this

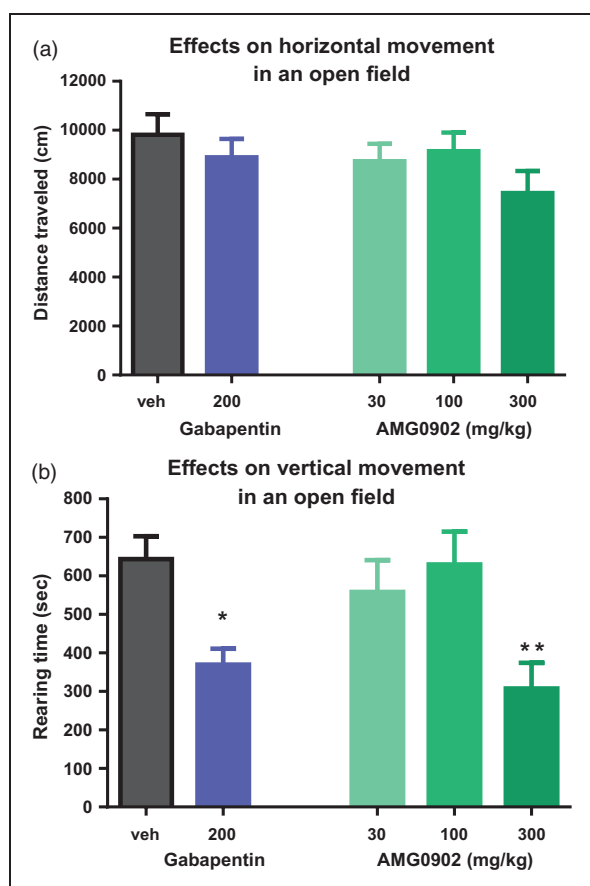


**Figure 3.** Open field analysis for the evaluation of the effect of AMG0902. (a) Sum of total distance traveled in centimeters during a 60-min observation. There was no significant effect of AMG0902. (b) Sum of total rearing behavior in seconds during a 60-min observation. There was a significant reduction of rearing following 200 mg/kg of gabapentin ( $p < 0.05$ ) as well as 300 mg/kg of AMG0902 ( $p < 0.01$ ).

assay, rats injected with CFA to one hind paw show a decrease in rearing behavior as measured 24 h later in an open field apparatus. This window of presumed hypersensitivity behavior can be reversed by standard non-steroidal anti-inflammatory drugs.<sup>29</sup> In addition to automated scoring, a key advantage of this model is that reduction of pain behavior is quantified as a recovery of normal rearing instead of a decrease in an evoked-response; thus, compounds that reduce general movement would not falsely be interpreted as efficacious. As demonstrated in Figure 4(a), there was a significant window of hypersensitivity as measured by the hind paw rearing time response of animals administered CFA ( $204 \pm 25$  s) as compared to vehicle control hind paw rearing time response ( $545 \pm 40$  s;  $t_{22} = 7.2$ ,  $p < 0.01$ ). There was an overall significant effect on hypersensitivity ( $F_{4, 55} = 3.8$ ) with the reduction in rearing inhibited by 3 mg/kg naproxen ( $418 \pm 49$  cm;  $p < 0.01$  by Dunnett's Multiple Comparisons; Figure 4(a)).

AMG0902 dosed at 100 mg/kg produced no significant effect on rearing time relative to vehicle ( $264 \pm 52$  s;  $p > 0.05$  by Dunnett's Multiple Comparisons; Figure 4(a)) despite a mean unbound plasma concentration of  $6.1 \pm 2.4 \mu\text{M}$ , which is  $>3$ -fold in excess of the in vivo  $\text{IC}_{90}$  calculated from the AITC target coverage model.

**Modest reversal of pressure threshold hypersensitivity.** Twenty-four hours after CFA injection into the left hind paw, the paw withdrawal thresholds of rats were determined using the Digital Paw Pressure Randall-Selitto Meter. Rats with a threshold of less than 60 g were included in the study. Three hours post-dosing of 2 mg/kg indomethacin and 2 h post-dosing of 300 mg/kg AMG0902, rats were again evaluated for mechanical hypersensitivity using the Digital Paw Pressure Randall-Selitto Meter. There was an overall significant effect on hypersensitivity ( $F_{2,36} = 25.0$ ) with the reduction in mechanical threshold inhibited by indomethacin ( $120 \pm 6.1$  g,  $p < 0.01$ ) relative to vehicle ( $69 \pm 2.7$  g; Figure 4(b)). There was also a significant effect on reduction of hypersensitivity by AMG0902 following 300 mg/kg ( $87.6 \pm 4.4$  g,  $p < 0.05$ ) but only a 21% reduction compared to the 50% reduction of indomethacin, Figure 4(b). The mean unbound plasma concentration was  $35 \pm 11 \mu\text{M}$  which is  $>20$ -fold in excess of the in vivo  $\text{IC}_{90}$  calculated from the AITC target coverage model.

#### AMG0902 did not reverse SNL-induced tactile allodynia

Two weeks after SNL surgery, control rats exhibited a tactile threshold of  $2.3 \pm 0.35$  g (1 h post-dosing of vehicle) and  $2.3 \pm 0.65$  g (2 h post-dosing of vehicle; Figure 4(c)). By Dunnett's Multiple Comparison Test relative to vehicle control, gabapentin significantly reversed SNL-induced mechanical allodynia with a significant increase in the threshold to  $5.7 \pm 1.4$  g (at the 1 h post-dosing test time;  $F_{3,36} = 2.28$ ,  $p < 0.05$  relative to vehicle by Dunnett's multiple comparisons test) and  $9.9 \pm 1.6$  g (at the 2 h post-dosing test time;  $F_{3,36} = 0.40$ ,  $p < 0.05$  relative to vehicle by Dunnett's multiple comparisons test). AMG0902 at 300 mg/kg p.o. produced nonsignificant effects on von Frey threshold relative to vehicle at either post-dosing test time ( $p > 0.05$  by Dunnett's multiple comparisons test) with tactile thresholds of  $2.0 \pm 0.33$  g and  $2.0 \pm 0.33$  g, respectively (Figure 4(c)). The mean unbound plasma concentration in this dosing group was  $8.4 \mu\text{M}$ , which is  $>4$ -fold in excess of the in vivo  $\text{IC}_{90}$  calculated from the AITC target coverage model. Similar to the results reported here, another potent and selective antagonist, A-967079 was also reported to be ineffective in reversing mechanical hyperalgesia in CCI, SNL, and CFA models of pain (Table 2 and Chen et al.<sup>42</sup>).

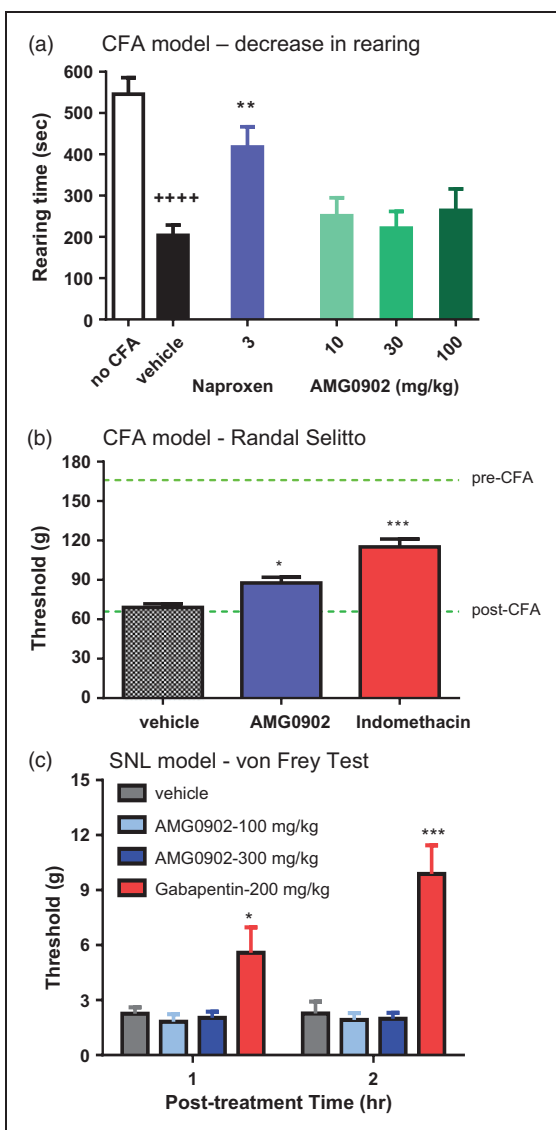


**Figure 4.** Behavioral models of mechanically activated hypersensitivity. (a) Sum of total rearing behavior in seconds during a 60-min observation that was 23 h post unilateral hind paw CFA injection. There was a significant reduction of rearing following CFA injection in animals orally dosed with vehicle ( $p < 0.0001$ ). There was a significant inhibition of the reduction in rearing with 3 mg/kg naproxen sodium ( $p < 0.01$ ) but no significant reduction with AMG0902 dosed up to 100 mg/kg. (b) CFA-induced model of mechanical hypersensitivity evaluated with a Randall Selitto device. AMG0902 dosed at 300 mg/kg produced a 21% ( $p < 0.05$ ) and indomethacin produced a 50% ( $p < 0.001$ ) reduction in hypersensitivity. Resulting mean unbound plasma concentration was  $35 \pm 11 \mu\text{M}$  which is  $> 20$ -fold in excess of the in vivo  $\text{IC}_{90}$  of AITC flinching. (c) Gabapentin significantly reversed SNL-induced mechanical allodynia at 1 h ( $p < 0.05$ ) and at 2 h ( $p < 0.001$ ), but there was no significant effect with AMG0902. The mean unbound plasma concentration in this dosing group was  $8.4 \mu\text{M}$  which is  $> 4$ -fold in excess of the in vivo  $\text{IC}_{90}$  of AITC flinching. CFA: complete Freund's adjuvant; SNL: spinal nerve ligation.

## Discussion

Here we report the in vitro and in vivo pharmacology of AMG0902, a potent and selective antagonist of TRPA1 channels. AMG0902 demonstrated significant TRPA1 antagonism in an in vivo target coverage model (AITC-induced licking/flinching in rats), and it significantly blocked high threshold mechanically induced activation of C fibers in situ. However, the effect of AMG0902 on pain behavioral models of inflammatory and neuropathic pain was not robust. AMG0902 was less efficacious than an NSAID in a model of CFA-induced mechanical hypersensitivity using a Randall Selitto device (with protein unbound plasma concentrations [exposure] that were 20-fold in excess of the in vivo  $\text{IC}_{90}$  from AITC flinching) and no efficacy was observed in a CFA model of reduced rearing behavior in an open field box<sup>29</sup> (exposure 3-fold in excess of the in vivo  $\text{IC}_{90}$  from AITC flinching). In a model of neuropathic pain, AMG0902 had no effect on SNL-induced tactile allodynia at plasma unbound concentrations in excess of 4-fold of the calculated in vivo  $\text{IC}_{90}$  from AITC flinching concentration in a TRPA1-specific target coverage model. This suggests that either TRPA1 does not play a meaningful role in mechanical pain behaviors measured or higher target coverage is required for efficacy. Here we discuss the results of this study in the context of antagonist exposure in vivo and TRPA1 function in different in vivo models.

### Comparison of exposure in different models: Relationship to target coverage and efficacy

Licking/flinching behavior induced by AITC represents an activation of TRPA1 receptors on C fibers, and such a response may only need activation of a small subpopulation of TRPA1 channels; hence, target coverage measured in the AITC model may be an underestimate relative to target coverage required in pain models in which TRPA1 channels are reportedly upregulated. A second potential underestimation could come from the way the AITC dose is chosen for an antagonist evaluation. Typically, an  $\text{ED}_{80}$  of an agonist dose is identified based on a dose-response relationship of a single, quantifiable behavior resulting from administration of the agonist. Which behavior is chosen and how to quantify it is decided during the model development. Appropriateness of the calculated  $\text{ED}_{80}$  as the dose to be given for subsequent prevention experiments with the antagonist is based on an assumption that the behavioral end-point (such as AITC-induced licking/flinching) is linear. However, behavioral end-points may not be linear for a variety of reasons including physical limitations, such as the number of seconds of licking/flinching that are possible for a rat to display within the measured time. This may result in an  $\text{ED}_{80}$  value that is too low to

**Table 2.** Summary of published TRPA1 antagonists in pain models.

Compound	Model	Measure	Dose administered	Efficacy	Reference	Comments
TCS 5861528	MIA	Paw edema	10 mg/kg, p.o.	Yes	Moilanen et al. <sup>33</sup>	
HC-030031	TNBS-IC	VMR to CRD	3 mg/kg × 3 times i.v.	Yes	Kogure et al. <sup>34</sup>	
ADM_12	TG-inflam	vF-facial allodynia	30 mg/kg, p.o.	Yes	Gualdani et al. <sup>35</sup>	TRPV1 & TRPA1
HC-030031	Radicular pain	MH, TH	10 µg, i.t.	Yes	Miyakawa et al. <sup>36</sup>	
HC-030031	CCI	MA, CA	100 mg/kg, i.p.	Yes	Pinheiro Fde et al. <sup>37</sup>	
HC-030031	Interstitial cystitis	Bladder hyperalgesia	300 mg/kg, i.p.	Yes	DeBerry et al. <sup>38</sup>	
ADM_09	Oxaliplatin	MH, CA	30 and 120 mg/kg, p.o.	Yes	Nativi et al. <sup>39</sup>	
Chembridge-5861528	Brennan	MH, TA	30 mg/kg, i.p.	Yes	Wei et al. <sup>40</sup>	
HC-030031	MIA	Weight bearing	100 mg/kg p.o.	No	Okun et al. <sup>41</sup>	
A-967079	CCI, SNL, CFA	MH	62 mg/kg, p.o.	No	Chen et al. <sup>42</sup>	
A-967079	MIA	Grip force	20.7 and 62 mg/kg, p.o.	Yes	Chen et al. <sup>42</sup>	
HC-030031	CFA, SNL	MH	100 and 300 mg/kg, p.o.	Yes	Eid et al. <sup>15</sup>	
API8	CFA, SNL	MH, CA	1 mM, 10 µl, intra-paw	Yes	Petrus et al. <sup>14</sup>	

Abbreviations: monoiodoacetate (MIA); trinitrobenzenesulfonic acid-induced colitis (TNBS-IC); viceromotor response (VMR); colorectal distension(CRD); trigeminal inflammation(TG-inflam); von Frey (vF); mechanical hypersensitivity (MH); thermal hypersensitivity (TH); chronic constriction injury (CCI); mechanical allodynia (MA); cold allodynia (CA); postsurgical skin incision (Brennan); tactile allodynia (TA); spinal nerve ligation (SNL); complete Freund's adjuvant

cover the target at 80% occupancy. This may be the case with AMG0902 in which an unbound plasma concentration 5.6-fold higher than the *in vitro* IC<sub>90</sub> provides apparent full target coverage *in vivo* (*in vivo* AITC model IC<sub>90</sub>). Additional possible sources of underestimation may occur due to issues of accessibility of AITC or AMG0902 to different compartments such as skin nerve terminals, or it could be that AMG0902 can access TRPA1 receptors relevant in the skin nerve preparation more readily than nerve fascicles relevant in a nerve injury model.

### TRPA1 role in mechanical sensitivity (mechanosensation)

The suitability of TRPA1 as a pain target based on its role in mechanosensation has previously been explored.<sup>43</sup> One key study found that firing rates of C-fiber nociceptors in exogenous skin-nerve preparations taken from TRPA1 KO mice were half that of WT mice.<sup>26</sup> Here, we replicated these data and confirmed that mechanically induced C-fiber action potential firing is reduced in TRPA1 KO mice, particularly at high threshold forces, thus validating the functional involvement of TRPA1 in mechanotransduction. In a previous report, mechanically induced responses were also decreased in high threshold Aδ-fiber mechanoreceptors at forces greater than 100 mN, yet there was no difference found in low threshold Aβ and D-hair mechanoreceptive fibers.<sup>26</sup> We extended these data to show that the potent and selective TRPA1 antagonist AMG0902 also attenuates mechanically induced C-

fiber action potential firing to a comparable extent as TRPA1 KO mice. Further studies with HC-030031 similarly implicate TRPA1 in high threshold mechanotransduction since this TRPA1 antagonist reduced mechanically evoked action potential firing in C-fibers.<sup>44</sup>

Although there is no direct evidence to link observations in *ex vivo* skin-nerve preparations to *in vivo* behavioral models of inflammatory and neuropathic mechanical hypersensitivity, there is consistency in the lack of effect at low-threshold forces in both skin-nerve and behavioral models. Since AMG0902 is similarly potent *in vitro* at rat or mouse receptors (see Table 1), potential species differences are not an added complication. In the rat neuropathic pain model, the average force exerted by von Frey fibers to evoke a behavioral response was on average 2–10 g which is approximately 20–100 mN of force, and this force is applied to the rat's hind paw across a fiber tip that is round and approximately 0.2–0.5 mm in diameter (fibers that deliver greater force have larger diameters). In the CFA-induced reduction in rearing model, the force on the rat's paw is more difficult to discern since we do not know how much of the weight of the animal is borne by each paw, nor the surface area of the paw upon which the force is exerted onto the glass platform. A rough calculation suggests that 20% of the rat's weight would be borne on the CFA-injected paw, which would translate to approximately 55–75 g (~550–750 mN) of force. Furthermore, the area of the paw upon which the force is exerted would be diminished since it is at least 5- to 20-fold larger than the surface area of the tip of the von Frey filament. Thus, once adjusting for the fact that this

force is applied over the unknown, though certainly larger area size of paw contact, the force per unit area applied by a CFA-injected paw would be comparable to that of a von Frey filament and would still be considered low threshold.

AMG0902 did produce a modest but significant reduction of CFA-induced mechanical hypersensitivity when assessed with a Randall Selitto device. The response thresholds with this device are from higher threshold mechanical forces of 60–120 g (~600–1200 mN) applied by the forceps device as it exerts a squeezing mechanical force concentrated through a 1.35-mm probe tip applied to the plantar surface of the paw. Our results in the skin-nerve assay in which application of AMG0902 significantly reduced mechanically evoked action potential firings in C fibers at greater than 100 mN of force (approximately 10 g), suggest that the modest effect of this compound observed with the Randall Selitto device in animals injected with CFA may be due to antagonism of TRPA1-mediated mechanosensation.

**TRPA1 role in inflammatory and neuropathic pain.** Based on the current results, it can be concluded that AMG0902 is not an effective modulator of mechanical hypersensitivity or tactile allodynia in standard inflammatory and neuropathic behavioral assays, despite good target coverage in vivo. Even the mild effect seen in CFA-induced hypersensitivity measured with Randall Selitto was achieved at a dose that was not completely devoid of open field effects and thus the possibility of a confound cannot be excluded. Similar to the current results, the potent and selective antagonist A-967079 had no effect on von Frey-evoked tactile allodynia in CFA or SNL models.<sup>42</sup> This is despite observations that A-967079 efficiently blocks AITC-induced licking/biting in vivo<sup>42</sup> and is able to reduce transmission of high-intensity mechanical stimuli to the spinal cord in an ex vivo preparation.<sup>45</sup> Furthermore, several studies have reported effects on mechanical pain behavior using first-generation TRPA1 antagonists such as HC-030031, and multiple reports have shown a reduced ability to detect mechanical stimuli at the behavioral level in TRPA1 KO animals. Given the strong evidence in support of TRPA1's role in mechanosensation and our own data indicating that AMG0902 is able to inhibit chemical activation of TRPA1 in vivo, one possible explanation for these differences is that different compounds could inhibit TRPA1 via binding at different sites. Indeed, recent structural analysis of TRPA1 indicates that A-967079 likely forms a wedge that prevents movement of domains that are critical for channel gating, while HC-030031 binds to a distinct site that prevents channel activation via an unknown mechanism.<sup>46</sup> Even so, if the effect of

antagonism at different sites is still a decrease in the cation flux, the mechanism would be the same.

Considering the fact that standards of care pain medications such as Neurontin<sup>®</sup>/Lyrica<sup>®</sup> and Cymbalta<sup>®</sup> are effective in rodent pain models (CFA and SNL) and potent and selective TRPA1 antagonists such as A-967079 and AMG0902 are not effective, we stopped our pursuit of TRPA1 antagonists as pain therapeutics. However, clinical trials evaluating GRC 17536 in painful diabetic neuropathy trials are ongoing (<https://clinicaltrials.gov/ct2/show/NCT01556152>) and clinical plans for HX 100 continue ([http://www.hydrabiosciences.com/pdf/press\\_releases/2015\\_04\\_14.pdf](http://www.hydrabiosciences.com/pdf/press_releases/2015_04_14.pdf)). Antagonists of TRPA1 may also still hold therapeutic promise in indications like respiratory diseases such as cough,<sup>47</sup> itch, and edema in certain inflammatory conditions.

### Acknowledgments

The authors would like to thank their colleagues Tom Kornecook and Jessica Able for their help and input.

### Author Contributions

SGL, CLS, BDM, and NRG participated in the research design while KDW advised on research designs. ADW, BDY, MZ, RY, and WW conducted the experiments. YT and MC supported dose preparations and exposure measurements; LS and SG-M supported SAR and AMG0902 synthesis; and SGL, CLS, BDM, and NRG wrote or contributed to the writing of the manuscript.

### Declaration of Conflicting Interests

The author(s) declared no potential conflicts of interest with respect to the research, authorship, and/or publication of this article.

### Funding

The author(s) received no financial support for the research, authorship, and/or publication of this article.

### References

1. McKemy DD. How cold is it? TRPM8 and TRPA1 in the molecular logic of cold sensation. *Mol Pain* 2005; 1: 16.
2. Garcia-Anoveros J and Nagata K. *TRPA1: handbook of experimental pharmacology*. Berlin: Springer, 2007, pp.347–362.
3. Kobayashi K, Fukuoka T, Obata K, et al. Distinct expression of TRPM8, TRPA1, and TRPV1 mRNAs in rat primary afferent neurons with delta/c-fibers and colocalization with trk receptors. *J Comparat Neurol* 2005; 493: 596–606.
4. Obata K, Katsura H, Mizushima T, et al. TRPA1 induced in sensory neurons contributes to cold hyperalgesia after inflammation and nerve injury. *J Clin Invest* 2005; 115: 2393–2401.

5. Garcia-Anoveros J and Duggan A. TRPA1 in auditory and nociceptive organs. In: Liedtke WB and Heller S (eds) *TRP ion channel function in sensory transduction and cellular signaling cascades*. Boca Raton, FL: CRC Press, 2007, pp.167–176.
6. Kosugi M, Nakatsuka T, Fujita T, et al. Activation of TRPA1 channel facilitates excitatory synaptic transmission in substantia gelatinosa neurons of the adult rat spinal cord. *J Neurosci* 2007; 27: 4443–4451.
7. Merrill AW, Cuellar JM, Judd JH, et al. Effects of TRPA1 agonists mustard oil and cinnamaldehyde on lumbar spinal wide-dynamic range neuronal responses to innocuous and noxious cutaneous stimuli in rats. *J Neurophysiol* 2008; 99: 415–425.
8. Bautista DM, Jordt SE, Nikai T, et al. TRPA1 mediates the inflammatory actions of environmental irritants and proalgesic agents. *Cell* 2006; 124: 1269–1282.
9. Kremeyer B, Lopera F, Cox JJ, et al. A gain-of-function mutation in TRPA1 causes familial episodic pain syndrome. *Neuron* 2010; 66: 671–680.
10. Frederick J, Buck ME, Matson DJ, et al. Increased TRPA1, TRPM8, and TRPV2 expression in dorsal root ganglia by nerve injury. *Biochem Biophys Res Commun* 2007; 358: 1058–1064.
11. da Costa DS, Meotti FC, Andrade EL, et al. The involvement of the transient receptor potential A1 (TRPA1) in the maintenance of mechanical and cold hyperalgesia in persistent inflammation. *Pain* 2010; 148: 431–437.
12. Trevisan G, Hoffmeister C, Rossato MF, et al. Transient receptor potential ankyrin 1 receptor stimulation by hydrogen peroxide is critical to trigger pain during monosodium urate-induced inflammation in rodents. *Arthritis Rheumat* 2013; 65: 2984–2995.
13. Katsura H, Obata K, Mizushima T, et al. Antisense knock down of TRPA1, but not TRPM8, alleviates cold hyperalgesia after spinal nerve ligation in rats. *Exp Neurol* 2006; 200: 112–123.
14. Petrus M, Peier AM, Bandell M, et al. A role of TRPA1 in mechanical hyperalgesia is revealed by pharmacological inhibition. *Mol Pain* 2007; 3: 40.
15. Eid SR, Crown ED, Moore EL, et al. HC-030031, a TRPA1 selective antagonist, attenuates inflammatory- and neuropathy-induced mechanical hypersensitivity. *Mol Pain* 2008; 4: 48.
16. Lennertz RC, Kossyryeva EA, Smith AK, et al. TRPA1 mediates mechanical sensitization in nociceptors during inflammation. *PLoS One* 2012; 7: e43597.
17. Meotti FC, Forner S, Lima-Garcia JF, et al. Antagonism of the transient receptor potential ankyrin 1 (TRPA1) attenuates hyperalgesia and urinary bladder overactivity in cyclophosphamide-induced haemorrhagic cystitis. *Chem Biol Interact* 2013; 203: 440–447.
18. Schenkel LB, Olivieri PR, Boezio AA, et al. Optimization of a novel quinazolinone-based series of transient receptor potential A1 (TRPA1) antagonists demonstrating potent in vivo activity. *J Med Chem* 2016; 59: 2794–2809.
19. Klionsky L, Tamir R, Gao B, et al. Species-specific pharmacology of Trichloro(sulfanyl)ethyl benzamides as transient receptor potential ankyrin 1 (TRPA1) antagonists. *Mol Pain* 2007; 3: 39.
20. Le Poul E, Hisada S, Mizuguchi Y, et al. Adaptation of aequorin functional assay to high throughput screening. *J Biomol Screen* 2002; 7: 57–65.
21. Gavva NR, Bannon AW, Hovland DN Jr, et al. Repeated administration of vanilloid receptor TRPV1 antagonists attenuates hyperthermia elicited by TRPV1 blockade. *J Pharmacol Exp Therapeut* 2007; 323: 128–137.
22. Kwan KY, Allchorne AJ, Vollrath MA, et al. TRPA1 contributes to cold, mechanical, and chemical nociception but is not essential for hair-cell transduction. *Neuron* 2006; 50: 277–289.
23. Gingras J, Smith S, Matson DJ, et al. Global Nav1.7 knockout mice recapitulate the phenotype of human congenital indifference to pain. *PLoS One* 2014; 9: e105895.
24. Koltzenburg M, Stucky CL and Lewin GR. Receptive properties of mouse sensory neurons innervating hairy skin. *J Neurophysiol* 1997; 78: 1841–1850.
25. Stucky CL, Koltzenburg M, Schneider M, et al. Overexpression of nerve growth factor in skin selectively affects the survival and functional properties of nociceptors. *J Neurosci* 1999; 19: 8509–8516.
26. Kwan KY, Glazer JM, Corey DP, et al. TRPA1 modulates mechanotransduction in cutaneous sensory neurons. *J Neurosci* 2009; 29: 4808–4819.
27. Dube GR, Lehto SG, Breese NM, et al. Electrophysiological and in vivo characterization of A-317567, a novel blocker of acid sensing ion channels. *Pain* 2005; 117: 88–96.
28. National Research Council Committee for the Update of the Guide for the Care and Use of Laboratory Animals. The national academies collection: reports funded by National Institutes of Health (*guide for the care and use of laboratory animals*). Washington, DC: National Academies Press (US) National Academy of Sciences, 2011.
29. Youngblood B, Hever G, Zhang M, et al. Validation of a novel, automated assay of inflammation-induced allodynia in rats. *Soc Neurosci Abstr* 2008; 468: 13.
30. Kim SH and Chung JM. An experimental model for peripheral neuropathy produced by segmental spinal nerve ligation in the rat. *Pain* 1992; 50: 355–363.
31. Chaplan SR, Bach FW, Pogrel JW, et al. Quantitative assessment of tactile allodynia in the rat paw. *J Neurosci Method* 1994; 53: 55–63.
32. Dixon WJ. Efficient analysis of experimental observations. *Annu Rev Pharmacol Toxicol* 1980; 20: 441–462.
33. Moilanen LJ, Hamalainen M, Lehtimaki L, et al. Urate crystal induced inflammation and joint pain are reduced in transient receptor potential ankyrin 1 deficient mice—potential role for transient receptor potential ankyrin 1 in gout. *PLoS One* 2015; 10: e0117770.
34. Kogure Y, Wang S, Tanaka KI, et al. Elevated H<sub>2</sub>O<sub>2</sub> levels in TNBS-induced colitis rats contributes to visceral hyperalgesia through interaction with the TRPA1 cation channel. *J Gastroenterol Hepatol* 2015; 31: 1147–1153.
35. Galdani R, Ceruti S, Magni G, et al. Lipoic-based TRPA1/TRPV1 antagonist to treat orofacial pain. *ACS Chem Neurosci* 2015; 6: 380–385.
36. Miyakawa T, Terashima Y, Takebayashi T, et al. Transient receptor potential ankyrin 1 in spinal cord

- dorsal horn is involved in neuropathic pain in nerve root constriction rats. *Mol Pain* 2014; 10: 58.
37. Pinheiro Fde V, Villarinho JG, Silva CR, et al. The involvement of the TRPA1 receptor in a mouse model of sympathetically maintained neuropathic pain. *Eur J Pharmacol* 2015; 747: 105–113.
  38. DeBerry JJ, Schwartz ES and Davis BM. TRPA1 mediates bladder hyperalgesia in a mouse model of cystitis. *Pain* 2014; 155: 1280–1287.
  39. Nativi C, Gualdani R, Dragoni E, et al. A TRPA1 antagonist reverts oxaliplatin-induced neuropathic pain. *Sci Rep* 2013; 3: 2005.
  40. Wei H, Karimaa M, Korjamo T, et al. Transient receptor potential ankyrin 1 ion channel contributes to guarding pain and mechanical hypersensitivity in a rat model of postoperative pain. *Anesthesiology* 2012; 117: 137–148.
  41. Okun A, Liu P, Davis P, et al. Afferent drive elicits ongoing pain in a model of advanced osteoarthritis. *Pain* 2012; 153: 924–933.
  42. Chen J, Joshi SK, DiDomenico S, et al. Selective blockade of TRPA1 channel attenuates pathological pain without altering noxious cold sensation or body temperature regulation. *Pain* 2011; 152: 1165–1172.
  43. Garrison SR and Stucky CL. The dynamic TRPA1 channel: a suitable pharmacological pain target? *Curr Pharmaceut Biotechnol* 2011; 12: 1689–1697.
  44. Kerstein PC, del Camino D, Moran MM, et al. Pharmacological blockade of TRPA1 inhibits mechanical firing in nociceptors. *Mol Pain* 2009; 5: 19.
  45. McGaraughty S, Chu KL, Perner RJ, et al. TRPA1 modulation of spontaneous and mechanically evoked firing of spinal neurons in uninjured, osteoarthritic, and inflamed rats. *Mol Pain* 2010; 6: 14.
  46. Paulsen CE, Armache JP, Gao Y, et al. Structure of the TRPA1 ion channel suggests regulatory mechanisms. *Nature* 2015; 525: 552.
  47. Mukhopadhyay I, Kulkarni A, Aranake S, et al. Transient receptor potential ankyrin 1 receptor activation in vitro and in vivo by pro-tussive agents: GRC 17536 as a promising anti-tussive therapeutic. *PLoS One* 2014; 9: e97005.